ELSEVIER

Thermochimica Acta 321 (1998) 133–141

thermochimica acta

Characterization of fly ash from municipal solid waste incinerators using differential scanning calorimetry

Massimo Tettamanti[a,*], Elena Collina[a], Marina Lasagni[a], Demetrio Pitea[a], Domenico Grasso[1,b], Carmelo La Rosa[2,b]

[a] *Dipartimento di Chimica Fisica ed Elettrochimica, via Golgi 19, 20133 Milan, Italy*
[b] *Dipartimento di Scienze Chimiche, viale A, Doria 8, 95125 Catania, Italy*

Received 27 February 1997; accepted 20 May 1998

Abstract

Endothermic (in the 30–300°C range) and exothermic (in the 300–500°C range) processes were identified through differential scanning calorimetry experiments on fly ash in an air atmosphere. The endothermic processes are thermodynamically controlled and include the desorption of organic compounds along with a phase transition. Instead, exothermic processes are kinetically controlled and include two distinct combustion reactions. Their nature was confirmed by the flatness in DSC scans performed in nitrogen. The apparent activation energies of the two reactions are in very good agreement with those previously obtained from kinetic studies. Based on these laboratory experiments, the energy balance of the thermal process on the fly ash was performed. © 1998 Elsevier Science B.V.

Keywords: DSC; Fly-ash thermal treatment; Incineration; TG

1. Introduction

The ash (fly ash) in flue gases from combustion in municipal solid waste incinerators (MSWIs) collected in the environmental control units, contains both particulate carbon and significant concentrations of many different classes of organic compounds. Among these, the polychlorinated dibenzo-*p*-dioxins (PCDD) and polychlorinated dibenzofurans (PCDF) have been demonstrated to be particularly dangerous for human health and the environment [1].

In recent years, most studies have been focused on PCDD and PCDF formation. Other, somewhat more abundant and less toxic compounds, have not been given much consideration. Moreover, degradation reactions were not so intensively investigated as the formation ones [2].

Therefore, attention has been focused on the thermal behavior of fly ash and on kinetic and energy studies of the main fly-ash reactions [3–5]. Fly ash, collected from electrostatic precipitator (ESP) hoppers of different modern MSWIs, were subjected to a number of experiments.

The thermal degradation rate of organic compounds was studied in batch experiments. A general parameter, total organic carbon (TOC), was used to follow the variation of reagent concentration with time [5–7].

*Corresponding author. Tel.: 00 39 2 26603252; fax: 00 39 2 70638129; e-mail: pitea@sg2.csrsrc.mi.cnr.it

[1]Fax: +39-95-580138; e-mail: dgrasso@dipchi.unict.it

[2]Same as in Footnote 1.

0040-6031/98/$ – see front matter
PII: S0040-6031(98)00452-3

The main reaction product in air was CO_2. Desorption processes were also evaluated [5]. The TOC versus time data were well fitted by deconvolution with a sum of two exponentials. The hypothesis of two independent simultaneous first-order reactions, named R1 and R2, was made [5]. According to the calculated rate constants and to the activation and thermodynamic parameters, both reactions are the combustion of organic carbon to CO_2 [5].

This paper presents the results of fly-ash characterization by differential scanning calorimetry (DSC) for a better comprehension of the processes involved during thermal treatment. Thermogravimetric Analysis (TG) was used to interpret the peaks in the DSC scans.

2. Reagents and materials

Silica gel (Merck, grade 60, 230–400 Mesh ASTM), indium (extra pure, Mettler), aluminium (extra pure, Mettler), silver (extra pure, Mettler) were used without further treatment. Alumel, μ-metal and trafoperm are commercial names of extra pure Mettler standards.

Fly ash was collected from the ESP hoppers of MSWIs in Denmark (FA1: Reno-Nord and FA2a and FA2b: Reno-Syd) and Italy (FA3: AMSA, via Zama, Milano). The samples were homogenized using a ball mill (Retsch, Model S1) operating with three 10 mm and two 20 mm diameter balls at 80 rpm for 25 min.

3. Analytical procedures

3.1. DSC

DSC measurements were performed with a DSC Mettler DSC20 interfaced with a TC10A processor for the digital signal and with an IBM XT computer for data accumulation. The DSC cell was previously calibrated for temperature, using indium, aluminium and silver as standard, and for energy, using indium as standard.

The third degree polynomial, used as the baseline to calculate the heat associated to each scan peak, included the specific heat dependence of each sample on temperature. Equal amounts (10–20 mg) of the samples and the reference, silica gel previously dried to 700°C, were placed in 160 ml aluminium capsules and introduced into the calorimeter. The temperature was stabilized to ±0.2°C. The root mean square (RMS) of noise in energy was 0.05 mW.

3.2. TG

The TG measurements were performed with a Mettler TG50 thermobalance interfaced with a TC10A processor for the digital signal and with an IBM XT computer for data accumulation. The data analysis and calculation of the derived curve (DTG) were performed with 'home-made' software. The temperature calibration was made using Curie points of alumel (149.3°C), μ-metal (392.4°C) and trafoperm (754.6°C). The accuracy of temperature and mass was ±2% and ±1 mg, respectively.

4. Results

4.1. DSC

The DSC analysis of the fly-ash samples was performed in both air and nitrogen, also using different scan rates. Owing to the heterogeneity of fly ash, sample reproducibility was tested by repeating the same run at least twice, for example, Fig. 1 shows the scans of three runs performed in air on FA3, from 25° to 500°C at a scan rate of 10°C min^{-1}.

4.2. Runs in air

The runs were performed from 30° to 500°C, with scan rates of 8, 10, 12 and 14°C min^{-1}. On FA2b, an additional run with a 6°C min^{-1} scan rate was performed.

Fig. 2 shows the scans of all the fly-ash samples (scan rate: 10°C min^{-1}) while Fig. 3 shows those of FA2b at various scan rates. In each scan, peaks corresponding to both exothermic and endothermic reactions were observed.

Table 1 shows the experimental temperature at the peak maximum, T, as well as the enthalpy value for each peak, ΔH.

For a better understanding of the processes involved during the scans, the deconvolution of the DSC profiles was performed by minimizing the RMS between the experimental and the calculated curve, using a

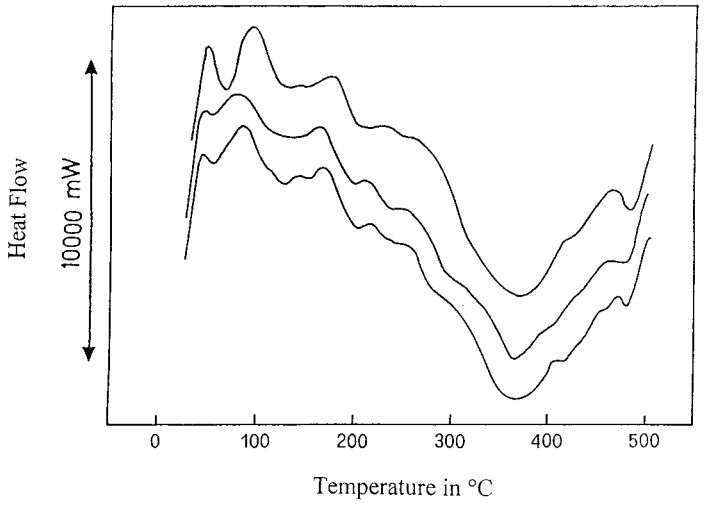

Fig. 1. Scans of three runs performed in an air atmosphere on FA3 to test the reproducibility, in the range 25–500°C, with a scan rate of 10°C min^{-1} (positive peaks correspond to endothermic phenomena).

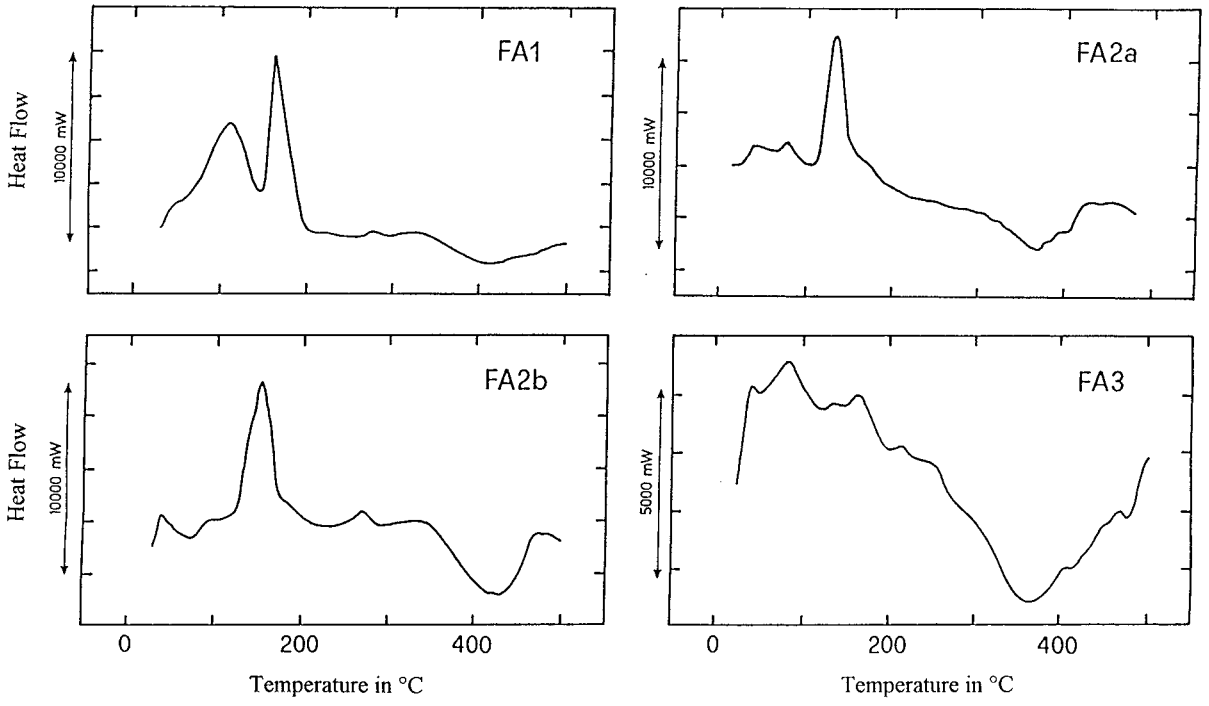

Fig. 2. Scans of runs performed on FA1, FA2a, FA2b and FA3 in an air atmosphere, in the range 30–500°C, with a scan rate of 10°C min^{-1} (positive peaks correspond to endothermic phenomena).

SIMPLEX type algorithm. The theoretical number of component peaks of a scan was defined by the minor number of Gaussian curves that gave a RMS of the same magnitude as the experimental error; Fig. 4 shows the reconstruction of the DSC profiles obtained with a scan rate of 10°C min^{-1}.

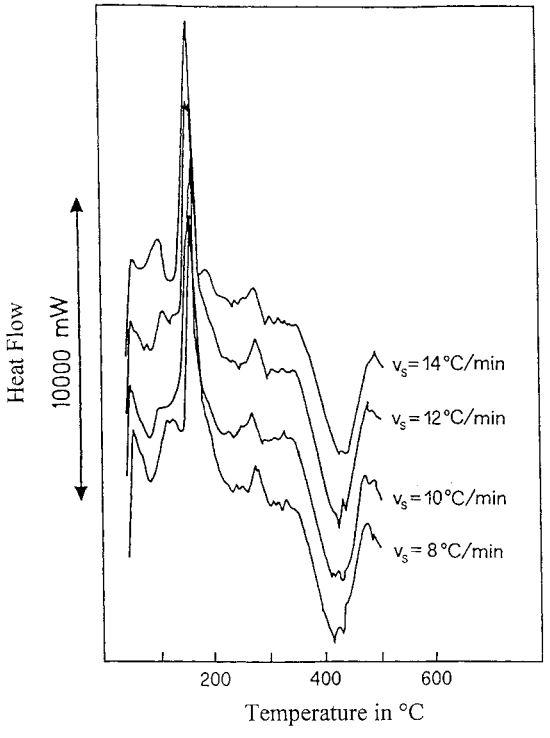

Fig. 3. Scans of FA2b in an air atmosphere, in the range 30–500°C, with scan rates of 8, 10, 12 and 14°C min^{-1} (positive peaks correspond to endothermic phenomena).

The accuracy of the fitting was estimated using the m parameter defined as

$$m = |\sum_i [(C_p^i)_{theor} - (C_p^i)_{exp}]/n| \quad (1)$$

where $(C_p^i)_{exp}$ is the ith value of the experimental, C_p, $(C_p^i)_{theor}$ the corresponding calculated value and n the total number of the scan points; in every fit the m value was <5%.

Table 2 shows the temperature and enthalpy of each peak resulting from deconvolution. It can be seen that the 'third' endothermic peak (apart from FA3 in air) and the exothermic peaks of FA1 and FA2a were deconvoluted as two Gaussians.

The reversibility of peaks was studied on FA1 (scan rate, 10°C min^{-1}; Fig. 5) and FA2a (14°C min^{-1}) using the following thermal path:

step 1 – heating of the sample from 30° to 250°C and subsequent cooling to 30°C;
step 2 – heating to 250°C and cooling to 30°C;
step 3 – heating to 500°C and cooling to 30°C; and
step 4 – heating to 500°C.

Moreover the FA3 sample, previously studied with a scan rate of 10°C min^{-1}, was re-analyzed in the 30–500°C range with a scan rate of 10°C min^{-1}.

The temperature dependence of the maximum of the deconvoluted exothermic peaks on the scan rate is reported in Table 3. From these data, the apparent activation energy, E_a, of the exothermic reactions, corresponding to the first (RE1) and the second (RE2) deconvoluted peaks, was calculated using equation [8]:

$$\ln(v_s/T^2) = C - E_a/RT \quad (2)$$

where v_s is the scan rate (°C min^{-1}), T the temperature (K) of the maximum of the peak, R the gas constant and C a constant. Table 4 shows the calculated E_a values.

The regression lines were obtained by a least-squares treatment and the goodness of fit is reported with the determination coefficient, r^2.

Table 1
Experimental parameters for DSC runs in air. Enthalpy value, ΔH, of each peak of the scans is given in J g^{-1}; temperature, T, at the peak maximum is given in °C (Temperature range=30–500°C)

Sample	Endothermic peaks						Exothermic peak	
	first [a]	second [a]	third [b]		fourth [a]			
	T	T	T	ΔH	T	ΔH	T [c]	ΔH
FA1	50±2	110±4	160±4	52±8	—	—	400±18	−(46±1)
FA2a	50±3	80±3	140±5	46±5	—	—	390±17	−(49±8)
FA2b	50±3	90±2	150±4	29±3	260±10	—	420±10	−(44±15)
FA3	50±6	80±5	160±5	12±3	—	—	360±17	−(75±1)

[a] ΔH not evaluated since no baseline was obtained.
[b] ΔH is the sum of two overlapping peaks.
[c] The temperatures are averaged because they are scan rate dependent.

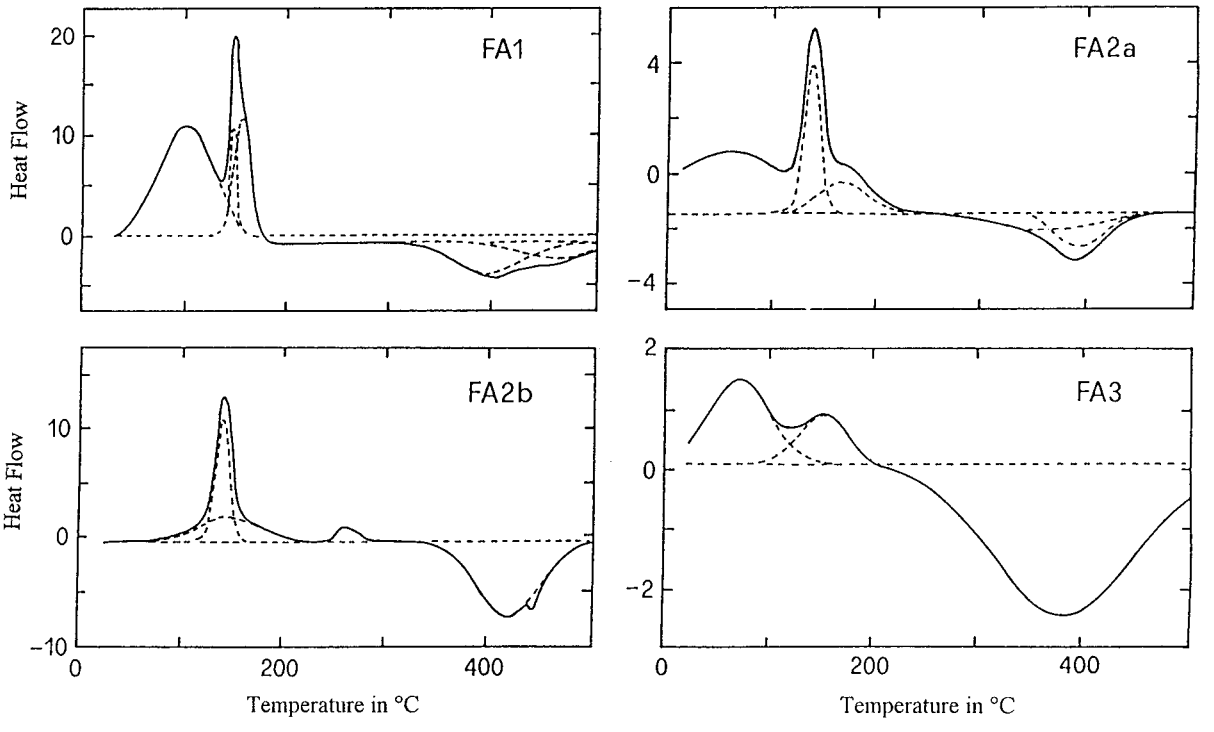

Fig. 4. Deconvolutions of experimental DSC profiles (solid lines) of FA1, FA2a, FA2b and FA3 (scan rate of 10°C min^{-1}).

4.3. Runs in nitrogen (pressure, 1.5 bar)

The dependence of peaks on reaction atmosphere was studied on a FA3 sample using the following thermal path, with a scan rate of 10°C min^{-1} (Fig. 6): step 1 – heating of the sample from 30° to 80°C, holding the temperature for 30 min and cooling to 30°C; and step 2 – heating to 500°C.

4.4. TG

A FA3 sample was analyzed by TG, with a 10°C min^{-1} scan rate, in air and in a nitrogen atmosphere (Fig. 7).

Table 2
Thermal characterization of deconvoluted DSC peaks (scan rate=10°C min^{-1}; temperature range 30–500°C). ΔH is given in J g^{-1}, T in °C

Sample	Endothermic peaks						Exothermic peak			
	second peak [a]		third peak [a]							
	irreversible		reversible		irreversible		irreversible			
	T	ΔH	T	ΔH	T	ΔH	T	ΔH	T	ΔH
FA1 [b]	100	124	146	12	155	40	389	−15	439	−31
FA2a [b]	58	—	137	24	167	22	328	−13	391	−36
FA2b [b]	—	—	141	17	149	15	—	—	420	−44
FA3 [b]	69	18	—	—	151	8	380	−75	—	—
FA3 [c]	—	—	163	14	248	8	—	—	—	—

[a] See Table 1.
[b] Runs in air.
[c] Run in nitrogen.

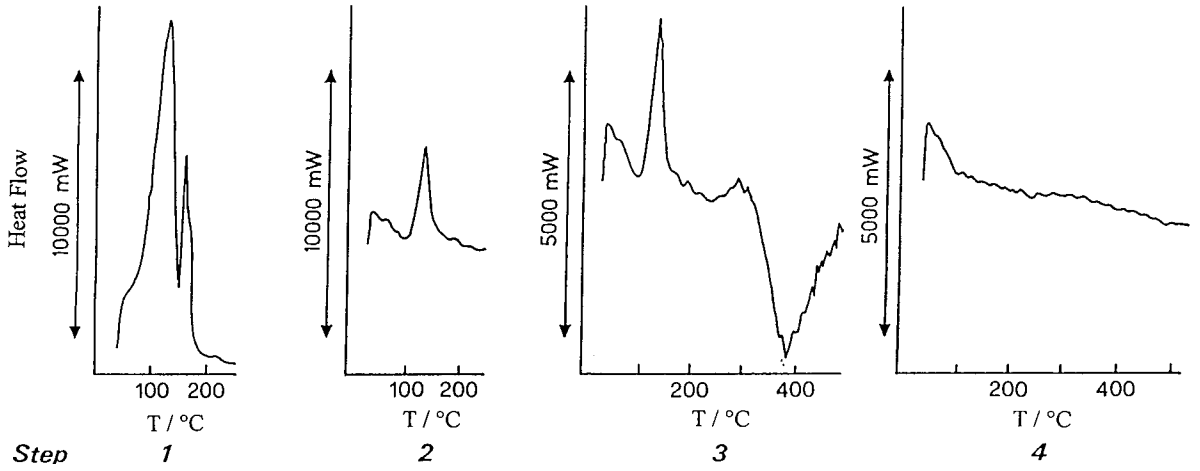

Fig. 5. Thermal path performed in an air atmosphere on FA1 to test the reversibility of peaks (scan rate of 8°C min^{-1}; positive peaks correspond to endothermic phenomena).

Table 3
Temperature dependence (°C) of the maximum of exothermic peaks on the scan rate (°C min^{-1}). RE1 and RE2 refer to the process involved in the first and second deconvoluted peaks, respectively

Scan rate	Sample				
	FA1	FA2a		FA2b	FA3
	RE1	RE1	RE2	RE1	RE1
6	—	376±4	390±3	—	—
8	392±3	380±2	396±4	410±2	351±4
10	406±5	390±4	401±3	414±4	367±4
12	418±4	405±2	—	422±4	373±5
14	427±4	407±3	—	423±2	377±5

5. Discussion

The results of the DSC analysis (Figs. 2 and 3) indicate a similar behavior for all samples, can be discussed in terms of the 30–300°C and 300–500°C temperature ranges.

5.1. Temperature between 30° and 300°C

This range was characterized by endothermic peaks whose position in the scans did not depend on the scan rate. Thus, these reactions were under thermodynamic control.

The scans of FA1 (Fig. 2) presented a shoulder at ca. 50°C and two well-defined peaks with maxima at 110° and 160°C. The scans of FA2a (Fig. 2) and FA2b (Figs. 2 and 3) presented three peaks at 50°, 80–90° and 140–150°C. From their position on the temperature scale and the relative height of the peaks at 50° and 140–150°C, it seems that they corresponded to FA1 peaks at 50° and 160°C. On the contrary, the peak at ca. 100°C was not so high as the corresponding

Table 4
Activation energies, E_a (kJ mol^{-1}) calculated from DSC data. The corresponding values obtained from kinetic studies are taken from [5]

Sample	DSC data				Kinetic data			
	RE1	r^2	RE2	r^2	R1	r^2	R2	r^2
FA1	30±6	1.00	—	—	27±8	0.68	18±7	0.53
FA2a	17±9	0.92	47±4	0.99	33±7	0.73	40±6	0.86
FA2b	108±9	0.95	—	—	83±7	0.98	29±4	0.95
FA3	48±4	0.92	—	—	49±5	0.95	51±3	0.98

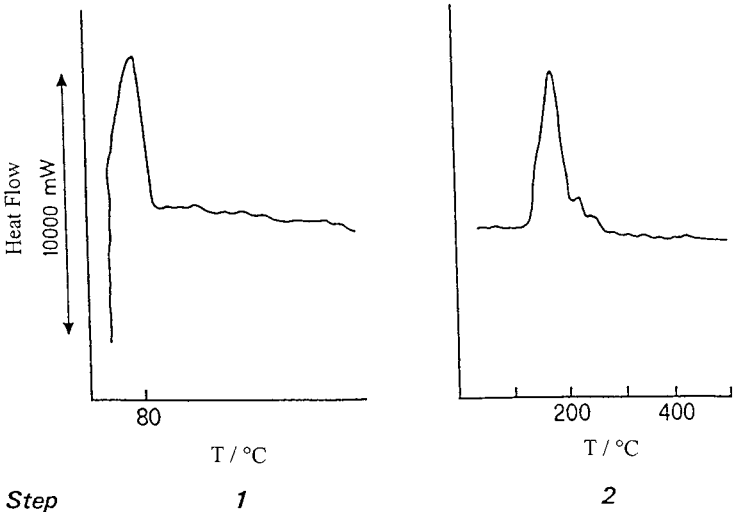

Fig. 6. Thermic path performed under nitrogen on FA3 to test the dependence of peaks on reaction atmosphere (scan rate of 10°C min^{-1}; positive peaks correspond to endothermic phenomena).

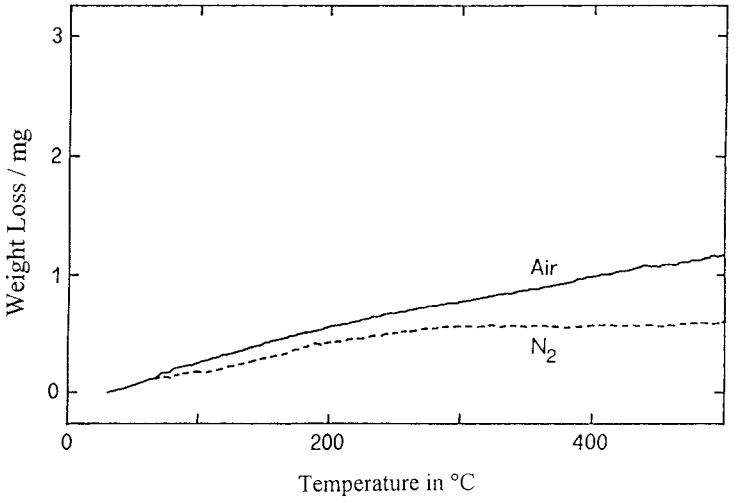

Fig. 7. TG performed in an air atmosphere and under nitrogen on FA3 (scan rate of 10°C min^{-1}).

FA1 peak. Moreover, the FA2b sample presented a peak at ca. 270°C.

Although, FA3 (Fig. 2) showed a much more complex behavior, nevertheless peaks were present at 50°, 80° and 160°C.

The scans obtained under nitrogen (Fig. 6), with preliminary treatment at 80°C for 30 min, did not present the endothermic peak at ca. 100°C. Thus, the hypothesis that this peak is due to water desorption seems to be reasonable.

In all the scans, the main peak fell ca. 150°C ($\Delta H \cong 50$ J g^{-1}). To clarify its nature, the thermal paths shown in Fig. 5 were performed. The following information was obtained from steps 1 and 2: the water peak disappeared, the 'main' peak being substantially unaltered in the temperature scale while the calculated enthalpy decreased ($\Delta H \cong 20$ J g^{-1}). In step 3, it was seen that this peak was reversible. The first heating to 500°C changed the sample completely. In fact, during step 4, no phenomenon was observed. This behavior

phenomenon can be interpreted in terms of two overlapping peaks as confirmed by the results of deconvolution of the profiles (Fig. 4): the peak is very well fitted using two Gaussian curves. The first is reversible, probably due to a phase transition of a compound on fly ash; the second is irreversible and probably due to the desorption of organic compounds. The hypotheses regarding these peaks are supported by the reaction products identification as well as the transition observed between two different 'structure organizations' in the fly-ash thermal degradation in air [5]. To obtain a more accurate description of the phenomenon, the non-linear deconvolution procedure was conditioned, with the condition that the area of the lower temperature component (120–150°C) of the peak should be equal to the measured experimental enthalpy of the reversible peak.

The other endothermic peaks, that were irreversible (Fig. 5) and not dependent on the reaction atmosphere (Fig. 6), were attributed to the desorption of organic compounds.

5.2. Temperature between 300° and 500°C

This range is characterized by the presence of a large exothermic peak whose position depends on the scan rate (Table 3); thus, the reaction was under kinetic control.

The deconvolution procedure (Fig. 4) resulted in two peaks for FA1 and FA2a but in only one for FA2b (with a residual area) and FA3. Due to the resolution of the two overlapped peaks, the temperature dependence of the maximum of both peaks on scan rate can be calculated only for FA2a (Table 4). Thus, two distinct processes, here named RE1 and RE2, are involved during the thermal oxidation of fly ash. This conclusion strongly supports our results from kinetic studies [5].

In Table 4, the apparent activation energies calculated from DSC data for RE1 and RE2 processes are compared with those obtained from kinetic experiments for R1 and R2 reactions. Looking at the values for FA2a, the processes RE1 and RE2 are, respectively, identical to reactions R1 and R2. On this basis, the good agreement between activation energies suggests that RE1 and R1 reactions for FA1 and FA2b are identical. By analogy, it is probable that the same identification is possible for FA3 but due to the non-significant difference (at 5% level) between activation energies for R1 and R2 reactions [5], it is almost impossible to arrive at a definite conclusion.

Moreover, the lack of peaks in the runs performed in nitrogen confirms that R1 and R2 are combustion reactions.

It must be noted that the enthalpy values (Table 1) make it possible to calculate the energy balance for the thermal treatment. For the global process at 500°C, the treatment of FA1, Fa2a and FA2b is substantially balanced whereas there is a gain of ca. 50 J g^{-1} for FA3.

Finally, owing to instrumental limits, the TG was not useful in the quantification of the organic compounds connected with each DSC peak. However, the quantitative experimental data allowed the calculation of the progressive weight loss together with the total weight loss as a function of the temperature and operative conditions. In particular, all the fly ash lost ca. 5% in weight.

6. Conclusions

DSC, coupled with the TG, supplies useful information for the characterization of phenomena tied to the release of substances when fly ash is exposed to heating up to 500°C, in air or nitrogen.

From the TG, a weight loss of ca. 5% was calculated for all the studied fly ash.

The DSC experiments in air allowed the identification of endothermic (in the 30–300°C range) and exothermic (in the 300–500°C range) processes. The first process includes the desorption of organic compounds as well as a phase transition. Instead exothermic processes are under kinetic control and include two distinct combustion reactions. The apparent activation energies of such reactions are in very good agreement with those obtained from kinetic studies. The lack of peaks in the runs performed in nitrogen confirms that the two reactions were combustible in nature.

Based on the laboratory experiments, the entire thermal inertization process seems to be balanced in as far as the energies of endothermic and exothermic reaction are concerned.

Acknowledgements

We wish to thank the Italian CNR (National Research Council) for its financial support (Grant no. 95.00522.CT13).

References

[1] D. Pitea, L. Bonati, U. Cosentino, M. Lasagni, G. Moro, Toxicol. Environ. Chem. 23 (1989) 239.
[2] E. Collina, M. Lasagni, D. Pitea, B. Keil, L. Stieglitz, Environ. Sci. Technol. 29 (1995) 577.
[3] E. Collina, M. Lasagni, M. Tettamanti, M. Mapelli, L. Forni, D. Pitea, Organohalogen Compd. 11 (1993) 265.
[4] M. Lasagni, E. Collina, M. Tettamanti, D. Pitea, Environ. Sci. Technol. 30 (1996) 1996.
[5] M. Lasagni, E. Collina, M. Tettamanti, D. Pitea, Environ. Sci. Technol., submitted for pubblication.
[6] M. Lasagni, E. Collina, M. Tettamanti, M. Ferri, D. Pitea, Organohalogen Compd. 11 (1993) 199.
[7] M. Lasagni, E. Collina, M. Ferri, M. Tettamanti, D. Pitea, Waste Management and Research 15 (1997) 507.
[8] J.M. Sánchez-Ruiz, J.L. López-Lacomba, M. Cortijio, P. Mateo, Biochemistry 27 (1988) 1648.